

Tapping mode microwave impedance microscopy

K. Lai,¹ W. Kundhikanjana,¹ H. Peng,² Y. Cui,² M. A. Kelly,¹ and Z. X. Shen¹

¹*Department of Applied Physics, Geballe Laboratory for Advanced Materials, Stanford University, Stanford, California 94305, USA*

²*Department of Material Science and Engineering, Stanford University, Stanford, California 94305, USA*

(Received 13 February 2009; accepted 1 April 2009; published online 27 April 2009)

We report tapping mode microwave impedance imaging based on atomic force microscope platforms. The shielded cantilever probe is critical to localize the tip-sample interaction near the tip apex. The modulated tip-sample impedance can be accurately simulated by the finite-element analysis and the result agrees quantitatively to the experimental data on a series of thin-film dielectric samples. The tapping mode microwave imaging is also superior to the contact mode in that the thermal drift in a long time scale is totally eliminated and an absolute measurement on the dielectric properties is possible. We demonstrated tapping images on working nanodevices, and the data are consistent with the transport results. © 2009 American Institute of Physics.

[DOI: [10.1063/1.3123406](https://doi.org/10.1063/1.3123406)]

I. INTRODUCTION

Near-field microscopy at microwave frequencies has attracted much research interest in the past decade.^{1,2} In order to obtain near-field images, it is crucial to keep close proximity between the probe and the sample during the scan. Due to the lack of feedback regulation on the tip-sample spacing, early implementations of microwave microscopes usually applied a large force up to 10^{-5} N to maintain the tip-sample contact.^{3,4} Such a strong contact force easily damages both the tip apex and the sample surface, preventing its applications on soft matter, nanoscale materials, and nanodevices. The advent of cantilever probes on atomic force microscope (AFM) platforms^{5–9} significantly alleviates the contact force down to 10^{-9} – 10^{-7} N, while detrimental effects inherent in contact mode AFM still exist. More importantly, a number of problems are associated with contact mode microwave imaging. First, a large background is present when measuring the reflected signal from the tip and common-mode cancellation is needed for signal amplification.⁸ The information obtained this way represents only the relative impedance change rather than the absolute local permittivity.⁹ In fact, modulation schemes are widely used in scattering near-field scanning optical microscopy (s-NSOM) to isolate the actual near-field signal from the background.¹⁰ Second, critical components in the microwave electronics, such as the rf source, the resonator, the 50 Ω impedance match, and the amplifiers, may drift in a long time scale due to temperature and other environmental variations. This becomes particularly problematic for careful experiments with long data acquisition times.

In this paper, we report the performance of tapping mode microwave impedance microscopy (MIM), utilizing the standard tapping mode operation in a commercial AFM. Since the cantilever probe, oscillating at its resonant frequency, only makes intermittent contact to the sample surface, tip wearing and sample dragging are greatly reduced.¹¹ Similar to the s-NSOM, the modulated microwave signal is an abso-

lute measurement of the local dielectric properties. Quantitative agreement between experimental data and simulation results were achieved on thin-film dielectric materials. Finally, because the actual tip-sample interaction is modulated at the tapping frequency,^{12,13} the slowly varying temperature and other electronic drifts, occurring in a much longer time scale, do not contaminate the microwave images. We have obtained tapping images on both test samples and working nanodevices.

II. EXPERIMENTAL SETUP

The experimental setup is schematically shown in the inset of Fig. 1. The cantilever probe is installed in a PacificNanotech¹⁴ AFM stage and the constant-amplitude tapping mode is employed. Our micromachined stripline probe¹³ is essential for this implementation. The shielded structure ensures that only the micron-sized focused-ion beam deposited Pt tip (Fig. 1 inset) interacts with the sample during the operation. Unshielded probes,^{8,15} on the other hand, are not suitable for tapping mode microwave imaging because of the overwhelming stray field contribution from the cantilever body. The mechanical resonant frequency f of the cantilevers is ~ 150 kHz and the quality factor $Q \sim 250$ in the ambient condition. Due to the complex layer structure, Q usually drops to ~ 50 when engaged on the sample surface. Future probe development will optimize the mechanical properties for better tapping functions.

The inset of Fig. 1 also illustrates the microwave (1 GHz) electronics, which detect small variations in the real (MIM-R) and imaginary (MIM-C) components of the tip impedance.⁹ A cancellation signal is provided to suppress the background so that small changes can be amplified without saturating the output. As detailed below, absolute dielectric information can still be recovered from the tapping operation. The mechanism of tapping mode MIM can be understood from the approaching curve (Fig. 1). As the tip vibrates sinusoidally above the sample surface, the tip-sample imped-

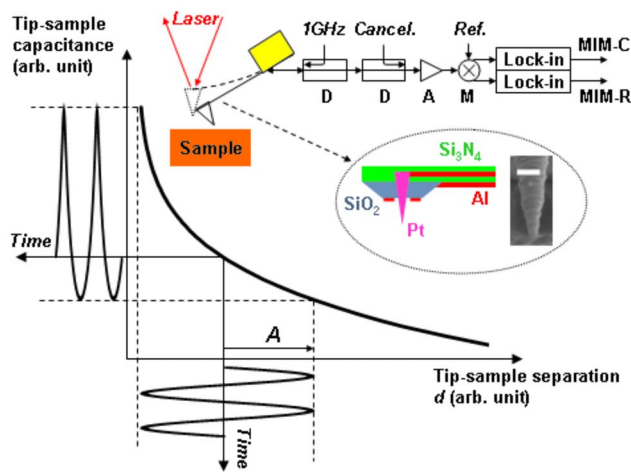


FIG. 1. (Color online) Tip-sample capacitance as a function of the spacing. As the tip oscillates above the sample surface, the tip impedance is also modulated at the same frequency. The inset shows the schematic of the tapping mode AFM and the microwave electronics (D—directional coupler, A—amplifier, M—mixer), as well as the cantilever structure and the SEM of the Pt tip. The scale bar is 500 nm.

ance is modulated at the same frequency. A lock-in amplifier referenced at this f can then measure the rms amplitude of the microwave signal. Only the first harmonic of the output is presented in the following, while higher harmonics can be measured if needed.

III. RESULTS AND DISCUSSIONS

Two sets of thin-film dielectric samples, plasma-enhanced chemical vapor deposited SiO_2 and Si_3N_4 films on heavily doped Si substrates ($\rho=0.01 \Omega \text{ cm}$), are measured using the tapping mode operation. The thickness t of the films nicely covers a range from 50 nm ($< \text{tip diameter } D$) to $1.5 \mu\text{m}$ ($> D$). The dielectric constants of the films, $\epsilon_r=4.5$ for SiO_2 and 6.2 for Si_3N_4 , are accurately determined before by a capacitance meter at 1 MHz.¹⁶ The same dielectric response is expected up to 1 GHz, as confirmed by earlier experiments.¹⁶ For each sample, the set point tapping amplitude $A=45 \text{ nm}$ ($f=134 \text{ kHz}$) is maintained for a few line scans and the MIM-C signals from the lock-in are recorded. The average MIM-C signal in Fig. 2, as expected, reduces with increasing film thickness. For a quantitative understanding, we employ a commercial finite-element analysis (FEA) software COMSOL 3.4 to simulate the tip-sample impedance.¹⁷ Details of the simulation are as follows. The tip geometry— $3 \mu\text{m}$ tall and $\theta=15^\circ$ —is taken from the scanning electron micrograph (SEM). A constant tip diameter $D=200 \text{ nm}$, close to the value before ($\sim 150 \text{ nm}$) and after ($\sim 220 \text{ nm}$) the measurement, is assumed in the simulation. For each film thickness t , the software generates a dense mesh, simulates the quasistatic potential distribution (Fig. 2 inset), and computes the tip-sample impedance at various separations d . For a sinusoidal tip motion, Fourier transform of the corresponding impedance was performed to extract the first harmonic signal. As seen in Fig. 2, excellent agreement between the modeling and the data can be achieved at $A=60 \text{ nm}$, larger than the nominal set point $A=45 \text{ nm}$. This

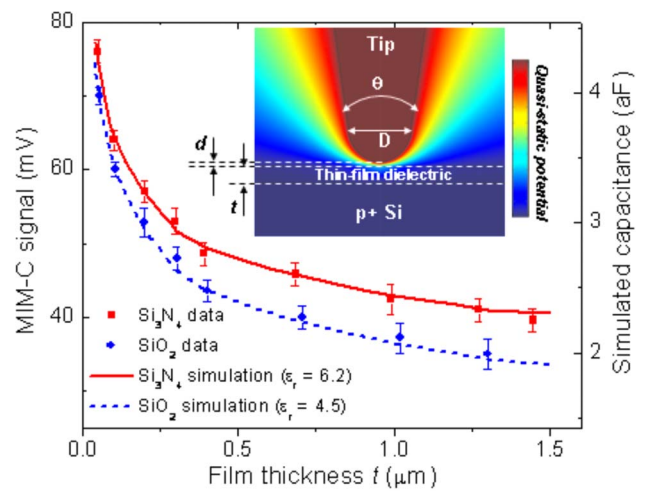


FIG. 2. (Color online) First harmonic MIM-C signal on several thin-film SiO_2 and Si_3N_4 samples. The FEA simulation results are also plotted for comparison. The inset shows the quasistatic potential distribution for a certain configuration—tip diameter $D=200 \text{ nm}$, tip-sample separation $d=10 \text{ nm}$, film ($\epsilon_r=6.2$) thickness $t=50 \text{ nm}$.

discrepancy may be explained by the fact that the laser spot is closer to the cantilever root than the actual Pt tip. The fitting also provides a good calibration to the MIM electronics so that 1 aF capacitance change in the tip corresponds to $\sim 18 \text{ mV}$ in the final output.

Using the standard feedback control for tapping mode AFM, dielectric variation in the sample can be quantitatively imaged. Figure 3(a) shows the sample structure for this experiment. A sputtered layer of Al_2O_3 ($\epsilon_r \sim 10$) covers a patterned SiO_2/Si wafer and the surface is polished, as seen in Fig. 3(b).⁸ The sample has been imaged in both contact and tapping modes by the same tip ($f=144 \text{ kHz}$, set point $A=30 \text{ nm}$, $D \sim 300 \text{ nm}$) at a scan speed of 5 s/line. During the long scan, appreciable electronic drift can be observed in the contact mode image, Fig. 3(c). Image processing is usually required to remove the slow-varying background drift, leaving only the relative dielectric contrast. The tapping mode image in Fig. 3(d), on the other hand, is clearly free

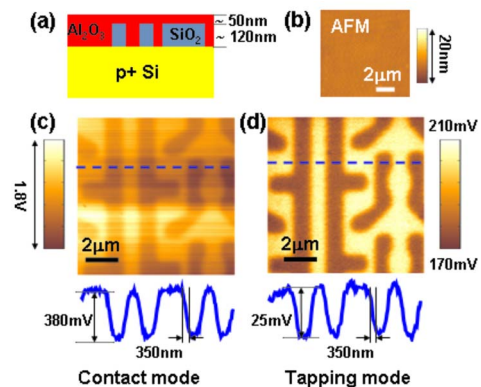


FIG. 3. (Color online) (a) Layer structure of the Al_2O_3 - SiO_2/Si sample. (b) AFM image of the polished sample surface. (c) Contact and (d) tapping mode MIM-C images taken by the same tip at the same area. The darker regions are buried SiO_2 . Electronic drift can be observed in (c) but not in (d). Line cuts are shown in both (c) and (d) for comparisons of the signal strength and the spatial resolution.

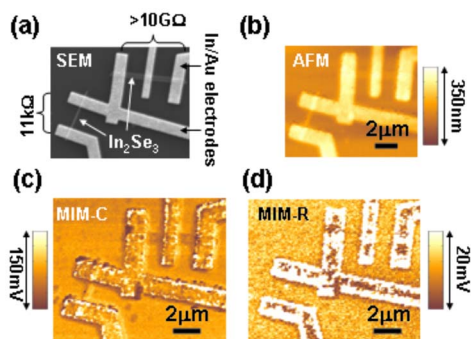


FIG. 4. (Color online) (a) SEM picture of In_2Se_3 nanoribbons and In/Au electrodes. The tapping data on the same devices are shown as (b) topography, (c) MIM-C, and (d) MIM-R images. The lower left device is more conductive than the one in the upper right.

from thermal drift because of the much faster sampling rate ($T=1/f$). Since the tapping MIM-C signal is an absolute measurement of the local dielectric properties, one can again simulate the structure and confirm that the thickness of extra Al_2O_3 on top of SiO_2 is about 50–100 nm. Figure 3 also includes a line cut in each image. The contact image exhibits higher contrast signal due to the continuous sampling and larger electronic gain, while both images show the same spatial resolution ~ 350 nm, which is defined by the tip diameter.

Finally, tapping mode images have been obtained, with little tip/sample damage, on real nanodevices. Figure 4(a) shows the SEM picture of two In_2Se_3 nanoribbons, contacted by In/Au electrodes, on a $\text{Si}_3\text{N}_4/\text{Si}$ substrate. Details of MIM studies on several In_2Se_3 devices have been reported elsewhere.¹⁸ Here we only qualitatively discuss the tapping data, Fig. 4(b)–4(d), measured by a different tip ($f=159$ kHz, set point $A=100$ nm). For the highly conductive device (two-terminal resistance $R\sim 10$ k Ω) on the lower left, the MIM-C signal is higher (brighter in the image) than that of the upper right one ($R>10$ G Ω). Indeed, when scanning on top of the conductive device, the tip is loaded by the capacitance between this conductor and the ground, resulting in a high MIM-C signal. For the resistive device, on the other hand, the tip is effectively lifted away from the $\text{Si}_3\text{N}_4/\text{Si}$ substrate by an insulator so the MIM-C signal is lower than that of the substrate. We note that, since the tapping motion effectively introduces a time varying capacitor in series with the sample impedance, the MIM-R channel output using conventional lock-in detection is dramatically suppressed. We are currently working on different electronic schemes to regain the full impedance information in the tapping mode.

In summary, we have demonstrated the tapping mode

operation of our microwave impedance microscope. The modulated near-field microwave response can be quantitatively simulated by FEA. Excellent agreement has been achieved between the modeling and the data on a set of thin-film dielectric samples. The tapping mode microwave imaging removes the thermal and other electronic drift observed in the contact mode. We also show that the tapping mode MIM can be performed on actual nanodevices.

The research is funded by Center of Probing the Nanoscale (CPN), Stanford University, a gift grant of Agilent Technologies, Inc., and DOE under Contract Nos. DE-FG03-01ER45929-A001 and DE-FG36-08GOI8004. This publication is also based on work supported by Award No. KUS-F1-033-02, made by King Abdullah University of Science and Technology (KAUST) under the global research partnership (GRP) program. CPN is an NSF NSEC, NSF Grant No. PHY-0425897. The cantilevers were fabricated in Stanford Nanofabrication Facility (SNF) by A.M. Fitzgerald and B. Chui in A.M. Fitzgerald & Associates, LLC, San Carlos, CA.

- ¹ B. T. Rosner and D. W. van der Weide, *Rev. Sci. Instrum.* **73**, 2505 (2002).
- ² S. M. Anlage, V. V. Talanov, and A. R. Schwartz, in *Scanning Probe Microscopy: Electrical and Electromechanical Phenomena at the Nanoscale*, edited by S. V. Kalinin and A. Gruverman (Springer, New York, 2006), pp. 207–245.
- ³ C. Gao, T. Wei, F. Duewer, Y. Lu, and X.-D. Xiang, *Appl. Phys. Lett.* **71**, 1872 (1997).
- ⁴ D. E. Steinhauer, C. P. Vlahacos, F. C. Wellstood, S. M. Anlage, C. Canedy, R. Ramesh, A. Stanishevsky, and J. Melngailis, *Appl. Phys. Lett.* **75**, 3180 (1999).
- ⁵ D. W. van der Weide and P. Neuzil, *J. Vac. Sci. Technol. B* **14**, 4144 (1996).
- ⁶ M. Tabib-Azar and Y. Wang, *IEEE Trans. Microwave Theory Tech.* **52**, 971 (2004).
- ⁷ T. Morita and Y. Cho, *Appl. Phys. Lett.* **84**, 257 (2004).
- ⁸ K. Lai, M. B. Ji, N. Leindecker, M. A. Kelly, and Z. X. Shen, *Rev. Sci. Instrum.* **78**, 063702 (2007).
- ⁹ K. Lai, W. Kundhikanjana, M. Kelly, and Z. X. Shen, *Rev. Sci. Instrum.* **79**, 063703 (2008).
- ¹⁰ R. Hillenbrand, T. Taubner, and F. Keilmann, *Nature (London)* **418**, 159 (2002).
- ¹¹ Q. Zhong, D. Inniss, K. Kjoller, and V. B. Elings, *Surf. Sci. Lett.* **290**, L688 (1993).
- ¹² A. Tselev, S. M. Anlage, H. M. Christen, R. L. Moreland, V. V. Talanov, and A. R. Schwartz, *Rev. Sci. Instrum.* **74**, 3167 (2003).
- ¹³ K. Lai, W. Kundhikanjana, M. Kelly, and Z. X. Shen, *Appl. Phys. Lett.* **93**, 123105 (2008).
- ¹⁴ Pacific Nanotechnology Inc. (now part of Agilent Technologies Inc.), Santa Clara, CA.
- ¹⁵ Scanning Microwave Microscopy probe, Agilent Technologies Inc., Santa Clara, CA.
- ¹⁶ Z. Wang, M. A. Kelly, Z.-X. Shen, G. Wang, X.-D. Xiang, and J. T. Wetzels, *J. Appl. Phys.* **92**, 808 (2002).
- ¹⁷ COMSOL, Inc., Palo Alto, CA.
- ¹⁸ K. Lai, H. Peng, W. Kundhikanjana, D. T. Schoen, C. Xie, S. Meister, Y. Cui, M. A. Kelly, and Z. X. Shen, *Nano Lett.* **9**, 1265 (2009).